

# A Walking Monitoring Shoe System for Simultaneous Plantar-force Measurement and Gait-phase Detection

Hui Yu, Dong-hai Wang, Can-Jun Yang, and Kok-Meng Lee, *Fellow, IEEE/ASME*

**Abstract**— This paper presents a walking-monitoring-shoe (WMS) system capable of simultaneously performing accurate plantar-force measurement and reliable gait-phase detection for continuous monitoring of human walking on treadmill. Based on anatomical information, the WMS employs four strain-gauges embedded in a homemade sole to accurately measure the contact force of the human foot exerted on the shoe-pad, and an efficient classification algorithm to detect five distinct gait-phases from the measured plantar force patterns. The WMS was experimentally evaluated, which has a typical 2<sup>nd</sup>-order system dynamics (with an 8% overshoot and a 2% settling time of 76ms when subject to a step input). Experimental results show that the accuracy and resolution of the sensing system are  $1.09 \pm 0.09\%$  (significant level=0.95) and 2N (0.2% of the maximal value of the load), respectively. The root-mean-square (rms) difference between the output signals of the WMS and the calibrated dynamic loading system was  $1.67 \pm 0.12\%$  (significant level=0.95). The feasibility of this integrated sensing/detection system was experimentally validated against video data, which relates gait-phases to the leg kinematics.

**Index Terms**— Gait, Force sensor, Instrumented shoe, Walking, Plantar force

## I. INTRODUCTION

Biomechanics of human walking has been an important multi-disciplinary research topic for many decades as humans rely on their feet daily. The science of walking requires the technology for gait analyses. Consistent measurements of ground reaction force (GRF) on human feet and cost-effective gait-phase detection (GPD) algorithms not only are potentially useful tools for practitioners in the clinical diagnoses and rehabilitation treatment [1], but also help researchers and scientists understand the biomechanics [2] and muscle coordination [3] of human walking for developing rehabilitation exoskeletons [4] as well as human-inspired mechanisms

(also known as humanoids) for robot walking [5].

Numerous systems have been developed for GRF assessment and can be broadly classified into two major categories; namely, ground mounted force platform and in- or instrumented shoes. Force platforms provide valuable information in studies on humans to measure GRF during walking or running; however, they offer little information about the force loaded on the specific anatomical region force plates [6], and are generally expensive. These disadvantages, along with the fact that the number of sequential ground-contact steps per trial is very limited, have motivated researchers to find cost-effective alternatives to force platforms for clinical applications. Instrumented shoes (capable of simultaneously measuring GRF-induced plantar forces and detecting gait-phases of human walking) emerge as an attractive alternative due to several outstanding merits including portability, flexibility and great convenience. Rapid advances in computer, mechatronic and MEMS-fabrication technologies further accelerate this trend, which enable manufacturing of high-performance sensors within small footprints widely available at low cost.

Instrumented shoes appeared as early as in 1873 as noted in [7] where a brief review of several other attempts (prior to 2002) can be found. In the mid-2000s, Veltink et al. [8] assessed plantar force using two sensors (forefoot and heel) in a sole configuration, while Faivre et al. [7] employed eight sensors in an instrumented sole. These instrumented shoes for plantar force measurements have not yet applied in gait analysis. Several different choices on the number and locations of force sensors were proposed to detect the gait phase [9]-[12]; for example, [9] used three force sensors (located at the heel, meta-1<sup>st</sup> and meta-4<sup>th</sup>) while [11] used four (with an additional sensor located at the hallux) to identify the gait phases with a classification algorithm, and have obtained good results.

Different sensing principles have also been widely explored for instrumented shoes. In the early designs, spring elements with strain gauges (under the heel and forefoot) were commonly used to measure vertical reaction and shear forces; (see for example [13]). F-san (Tekscan Inc., USA) utilizes force sensitive resistors [14]. Although they show the advantages in terms of portability, the sensor unit is difficult to calibrate for the reason that it can bend during the initial and late portions of the stance phase; and the physical characteristics of the twisted sensor are different from the flat. It also allows the foot to slip forward off of the insole

Manuscript received February 13, 2010. This work was supported in part by the Science and Technology department of Zhejiang Province Grant 2007C21G2010092.

Hui Yu, Dong-hai Wang, and Prof. Can-Jun Yang are with the Institute of Mechatronic and Control Engineering, the State Key Laboratory of Fluid Power Transmission and Control, Zhejiang University, 310027 P. R. China (phone/fax: 86-571-87953759; e-mail: yuhui\_1029@zju.edu.cn, ycj@zju.edu.cn).

Prof. K.-M. Lee is with the George W. Woodruff School of Mechanical Engineering, Georgia Institute of Technology, Atlanta, GA 30332-0405, USA (e-mail: kokmeng.lee@me.gatech.edu), and is visiting Pao Yu-Kong Chair Professor at the Zhejiang University.

due to the smooth surface. Experimental evaluation of an F-scan system [15] suggested that it lacks durability and suffers significant calibration error, and may not be entirely suitable for accurate and repeatable in-shoe measurements. Thin-film capacitance transducer matrix is commonly used in commercialized measurement device (for example, Pedar in-shoe system by Novel gmbh, Germany) for measuring vertical forces, which has the advantage of the ability to calibrate each individual sensor in the matrix. An earlier evaluation [16] on Pedar as a pressure measuring system with a built-in sensitivity threshold suggests that areas with small pressures can be missed. More recently, Kong and Tomizuka [17] installed air bladders and air pressure sensors for ground contact force measurement and proposed a fuzzy-logic algorithm to provide smooth and continuous detection of human gait phases to avoid problems of detecting low pressure signals by a threshold method. Fuzzy logic methods provide smooth outputs but tend to sacrifice response speed of the gait phase detection. It is also difficult to formulate fuzzy logic rules and assign values to critical parameters.

Over the last decade, numerous in-shoe devices (for examples, [9] - [11]) were proposed for gait data acquisition. These devices generally utilize plantar pressure signals measured by commercial sensors such as Flexiforce sensor (Tekscan Inc., USA) or FSR sensor (Interlink Electronics, USA). However, many of these published solutions are not suitable for precise plantar-force measurements due to the force sensor characteristics and/or the shoe structure [12][18], and commercial solutions (such as in-shoe pressure distribution of F-scan or Pedar systems) are expensive.

This paper presents an alternative sensing system for continuous monitoring of human walking by simultaneously measuring the plantar force and detecting the gait phases. Along with an efficient classification algorithm that detects five distinct gait-phases from plantar force patterns, a walking monitoring shoe (WMS) employing four force sensors embedded in a homemade sole has been developed for measuring the contact force on the shoe-pad. Three sets of experimental results are provided. The first two sets evaluate the performances of the WMS static/dynamic behaviors and the gait-phase detection algorithm. The third set validates the integrated sensing/detection method by relating the measured plantar forces and detected gait-phases to the joint kinematics of the leg.

## II. DESIGN OF A WALKING MONITORING SHOE (WMS)

The equation of motion for characterizing the dynamics of a human leg (Fig. 1) can be written as

$$\Gamma(\phi, \dot{\phi}) = \tau_{act} + \tau_e - \tau_f - \tau_T \quad (1)$$

where  $\phi$  is the joint-angle vector;  $\tau_{act}$  characterizes for the resultant force/torque exerted by the surrounding bones and

tissues (muscle and ligament);  $\tau_f$  is the joint friction force/torque; and  $\tau_T$  is the force/torque acting on the supporting leg from the ground reaction force. With rehabilitation applications in mind, we include  $\tau_e$  to account for the force/torque exerted by an external device (such as an exoskeleton).

In (1), the left-hand side accounts for the net effect of the leg inertia, the interaction between the rates of the translational and rotational within the biological knee joint and the gravity. As shown in Fig. 1(a), feet transfer the body weight to the ground during stance and walk. To provide a means for generating a model-based adaptive trajectory for controlling a rehabilitation exoskeleton [4], the effect of the ground reaction force/torque vector  $\tau_T$  (that varies from individual to individual as human walks with a unique gait pattern) must be well understood.

Although the bones making up the human feet through which the body weight is supported are complex skeletal structures, human feet have soft tissues that are compliant to the ground surface. As a result, the plantar pressure is uniformly distributed at contact areas as shown in Fig. 1(b) where Meta 1<sup>st</sup>, 2<sup>nd</sup>, and 4-5<sup>th</sup> mean the first, second, fourth and fifth metatarsals. The effect of  $\tau_T$  on the leg dynamics requires the determination of its instantaneous contact areas, ground reaction force, and the gait pattern of the walking.

### A. Factors influencing WMS Design

Although the gait pattern of each individual walking can be characterized by its own set of parameters (gait period, step length and joint angle), abnormal or comfortable gaits follow a universal law [20] dividing a gait cycle into eight phases that depend on the joints angles of the lower extremity as illustrated in Fig. 2 that shows the dependency of the plantar force distribution on the contact condition between the feet and ground during a gait cycle.

With the interest to develop a model-based adaptive trajectory algorithm for a rehabilitation exoskeleton in mind [4], the classification of the gait phases is reduced to a mapping relating the plantar force patterns among five phases during a gait cycle; initial contact (IC), mid stance

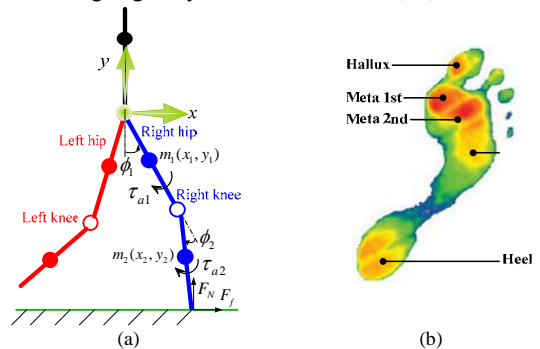


Fig. 1 Effect of feet reaction on leg dynamics. (a) Schematics illustrating the leg dynamic model. (b) Plantar pressure distribution [21].

(MS; including loading response), terminal stances (TS), pre-swing (PS) and swing phase (SP).

As illustrated in Figs. 1(b) and 2(b), the heel, metatarsals and hallux are the primary regions to bear the body weight [19]. The WMS is designed to have four force sensors configured at the heel, Meta 4-5<sup>th</sup>, Meta 1<sup>st</sup>, and hallux to measure plantar force and detect gait phase. Due to the closeness and relatively uniform pressure between the 1<sup>st</sup> and 2<sup>nd</sup> metatarsals, only one sensor is located at Meta 1<sup>st</sup>. The mapping between the plantar force patterns and gait phases can be best described in Table 1, where  $i=1, 2, 3$  and 4 correspond to the  $i^{\text{th}}$  force located at the heel, meta 4-5<sup>th</sup>, meta 1<sup>st</sup> and hallux respectively;  $\theta_i$  is a binary number denoting the state of the  $i^{\text{th}}$  sensor.

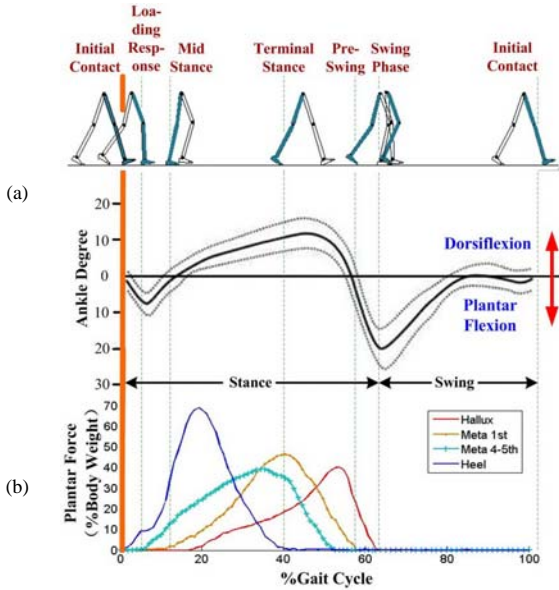


Fig. 2 Characteristics of the gait phases during a gait cycle. (a) Gait phases [20] in terms of ankle degrees. (b) Plantar forces at hallux, meta 1<sup>st</sup>, meta 4-5<sup>th</sup> and heel during walking (data from [7]).

TABLE 1 CORRESPONDENCE BETWEEN PLANTAR FORCE AND GAIT PHASE

Phase	Heel, $\theta_1$	Meta 4-5 <sup>th</sup> , $\theta_2$	Meta1 <sup>st</sup> , $\theta_3$	Hallux, $\theta_4$
IC	1*	0	0	0
MS	1	1	-	-
TS	0	-	1	-
PS	0	0	0	1
SP	0	0	0	0

\* The symbols 1, 0 and - denote “pressed”, “not pressed” and “not used” respectively.

### B. WMS Prototype Design

Figure 3 schematically illustrates the design of a WMS, which consists of four strain-gauge sensor assemblies sandwiched between the shoe-pad and sole, a signal processing circuit board for amplifying and filtering the analog force sensing signals, and a gait detection algorithm implemented on a host computer. As illustrated in Fig. 3(c), each of the four strain gauges (that simultaneously measure the plantar forces and identify the gait phase) is mounted

between a pair of aluminum plates and recessed to the sole to eliminate potential adverse effects due to the deformation of the sole (designed to absorb mechanical shocks) on the sensors.

In addition to being comfortable and easy to don and doff, the shoe-pad must be designed such that measurements of the force (acting by the foot on it during walking) have a reasonably good dynamic range, and that when the shoe-pad is loaded, the force transmits directly and perpendicular to the sensors. For this purpose, the shoe-pad has a flange to prevent horizontal translation, and thus minimize the effect of horizontal friction between the foot and shoe-pad on the sensor. The contacting surface between the flange and the sole is treated to allow smooth motion vertically by reducing friction between them.

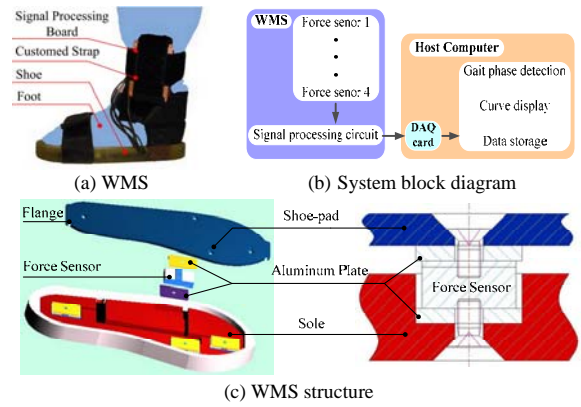


Fig. 3 WMS design schematics

### C. Gait Phase Detection Algorithm

Mathematically, Table 1 can be characterized by (2):

$$IC = \theta_1 \times \bar{\theta}_2 \times \bar{\theta}_3 \times \bar{\theta}_4 \quad (2a)$$

$$MS = \theta_1 \times \theta_2 \quad (2b)$$

$$TS = \bar{\theta}_1 \times \theta_3 \quad (2c)$$

$$PS = \bar{\theta}_1 \times \bar{\theta}_2 \times \bar{\theta}_3 \times \theta_4 \quad (2d)$$

$$SP = \bar{\theta}_1 \times \bar{\theta}_2 \times \bar{\theta}_3 \times \bar{\theta}_4 \quad (2e)$$

where  $\bar{\theta}_i$  is the complement of  $\theta_i$  (or  $\theta_i + \bar{\theta}_i = 1$ ). Built upon (2), an algorithm for detecting the gait-phase has been developed by defining a threshold  $\xi$  on the measured force  $f_i$  such that the binary output  $\theta_i$  is determined from (3):

$$\theta_i = \begin{cases} 1 & f_i > \xi \\ 0 & 0 < f_i \leq \xi \end{cases} \quad (3)$$

$$\xi = \lambda / P + \eta \quad \text{where } 0 < P \leq 1 \quad (4)$$

In (4),  $\lambda$  is the measured value without any load at the shoe;  $\eta$  represents an offset for regulating the sensitivity; and  $P$  is a stability function with respect to the state of the subject's body. As illustrated in Fig. 4, the measured  $\lambda$  provides a means to account for several environmental effects (such as zero shift, temperature shift and noise interference of the workplace), while  $\eta$  can be used to adjust the sensitivity of

the detection; the smaller the  $\eta$  value the higher is the detection sensitivity (to noise). It is expected that tremble and muscle spasm of the subject during walking can also influence the threshold value. With this in mind, the stability function  $P$  is included in (4) for future studies. For a normal subject,  $P=1$ .

The detection is executed in three steps:

*Step 1:* Calculate the threshold  $\zeta$  based on the walking condition and sensitivity requirement from (4).

*Step 2:* Given  $\zeta$ , calculate  $\theta_i$  by (3).

*Step 3:* Get the phase information from (2a-e).

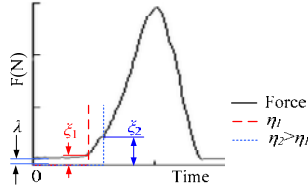


Fig. 4 Parameters affecting the threshold on the measured force

### III. EXPERIMENTAL RESULTS (VALIDATION)

A prototype WMS (Fig. 5) with four (XH32B-100) strain-gauge sensors (LZX S&T Inc., China) has been fabricated to measure the plantar force and detect the gait phase. Sensor specifications are given in Table 2.

TABLE 2 VALUES OF THE FORCE SENSOR PARAMETERS.

Dimension (L, W, H), mm	(30, 20, 10)	Mass, grams	30
Range, kN	1	Linearity, %	0.34
Overload, kN	1.5	Repeatability, %	0.31
		Hysteresis, %	0.26

The following experiments were performed:

- Estimate the force measuring properties of the WMS.
- Evaluate the threshold algorithm for gait-phase detection.
- Relate plantar forces, gait phases and joint kinematics.

#### A. Force measuring properties of the WMS

Experiments were performed to investigate the static and dynamic behaviors of the WMS for measuring forces. Static tests were carried out to determine the resolution and accuracy of the WMS using a set of step loads up to 900N (in step of 100N) generated by a Zwick/Roell Z2.5. The dynamic force measuring characteristics of the WMS was evaluated on a dynamic loading system (Fig. 5(b)) with a Tectis 3550 force transducer, through which the frequency and magnitude of the load can be adjusted. The sampling rate of the signals from the WMS and force transducer was individually set to 100Hz, and their output signals were collected simultaneously in response to a step load.

As shown in Fig. 5, the force transducer measures the vertical resultant force acting on the wooden foot model and thus its output  $F_t$  can be written as:

$$F_t = F_s + G_c + G_f + F_i \quad (5)$$

where  $F_s$  is the resultant output of the WMS;  $G_c$  is the gravitational force at the connector between the force

transducer and foot model;  $G_f$  is gravity of the foot model; and  $F_i$  is the total inertial force. The loading system, wooden foot model and shoe-pad are treated as rigid and thus, the inertial force  $F_i$  is neglected. The WMS exhibits typically a 2<sup>nd</sup> order response to the step load. The experimentally obtained static performance and step response characteristics of the WMS are summarized in Table 3. The WMS has a force-measuring accuracy of 1.09% and a 2% settling time of 76ms. From the maximum overshoot of 8.1% at  $t_p=45$ ms, the damping ratio  $\xi$  and natural frequency  $\omega_n$ , of the force-measuring system is approximately 0.625 and 89.43 rad/s respectively.

To evaluate the WMS dynamic performance to arbitrary loads, a time-varying load (created by adjusting the frequency and magnitude of the dynamic loading system) was applied to the WMS force measurement. Figure 6 compares the WMS output against the force-transducer signal, which agree well within 4% difference. The maximum absolute difference is 21.5N. The rms difference between the output signals of the WMS and loading system is  $1.67 \pm 0.12\%$  (significant level=0.95).

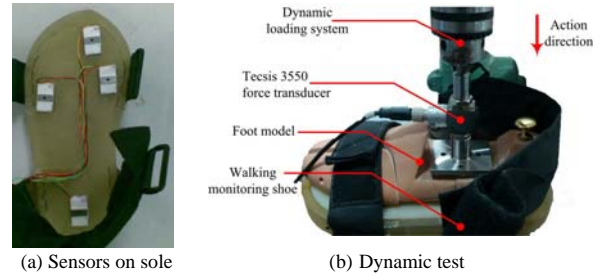


Fig. 5 Prototype WMS and dynamic loading system. The wooden foot model used has the same anatomic characteristics with human foot.

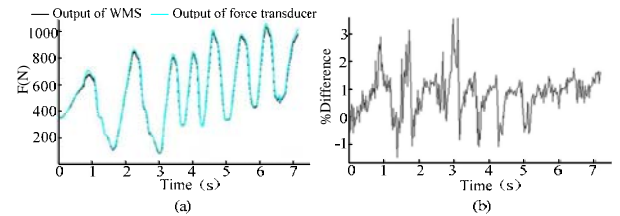


Fig. 6 Comparison of measured force to time-vary load. (a) Output signals of the WMS and force transducer. (b) % difference between WMS and force transducer.

TABLE 3 RESULTS OF FORCE-MEASURING PROPERTIES OF THE WMS

Parameter	Static test		Step response	
	Values	Transient	Data	
Resolution, N	2	$M_p$ , %	8.1	
Accuracy, %	1.09	$t_r$ , $t_p$ , $t_s(2\%)$ , ms	29, 45, 76	
Max. abs. error, N	16.5	$\xi$	0.625	
Max. rel. Error, %	4.57	$\omega_n$ , rad/s	89.43	

#### B. Gait phase detection

An off-line gait-phase detection algorithm has been written in Matlab for investigating the effects of the threshold  $\zeta$  on the gait phase detection. Twelve (19-31 years

old) subjects (2 females and 10 males with a weight range of 492-753N) with normal gaits participated in the experiments that were performed on a treadmill to evaluate the performance of the gait-phase detection algorithm. The subjects have no known pain or impairment that could influence their natural gait, and thus the stability function  $P=1$ . Over 40 trials (following the three detection steps discussed in Section IIC) were performed. A typical set of results are given in Figs. 7, 8 and 9, and Tables 4 and 5.

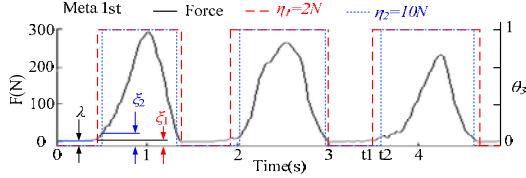


Fig. 7 Effect of different  $\eta$  values on the threshold  $\zeta$  and binary output  $\theta_3$ .

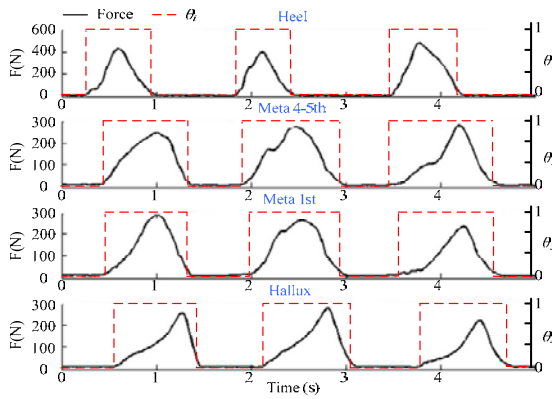


Fig. 8 Outputs of the WMS and the binary output  $\theta_i$  during three steps. Treadmill speed=2km/h,  $P=1$ ,  $\eta=5N$ .

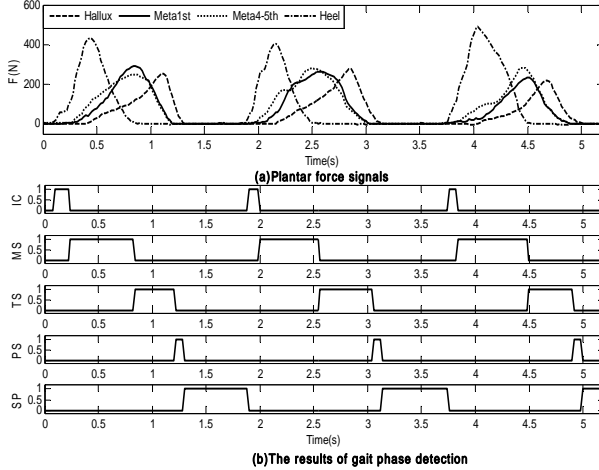


Fig. 9 Plantar forces and detected gait-phases. Speed=2km/h,  $P=1$ ,  $\eta=5N$ .

Observations from these results are discussed as follows:  
(1) Figure 7 illustrates the effect of two different  $\eta$  values (2 and 10N) on the threshold  $\zeta$  and on the binary output  $\theta_3$  of Meta 1<sup>st</sup> sensor. Consider the particular interval  $t=[3s, t_2]$  in Fig.7 as an illustration, where the measured no-load value  $\lambda$  of Meta 1<sup>st</sup> sensor changes somewhat due to noise. With the

sensitivity regulator  $\eta$  set at 2N (corresponding to the sensor resolution), the algorithm thresholds  $\theta_3=1$  at  $t=t_1$  although a more reasonable time to trigger-on ( $\theta_3=1$ ) is somewhere between  $t_1$  and  $t_2$ ; the latter corresponds to  $\eta=10N$ . With experimental trials—and-errors, the sensitivity regulator is set to  $\eta=5$  as a compromise between detection accuracy and immunity to no-load noise in the subsequent experiments.

(2) Figure 8 shows the plantar forces measured by the WMS and their calculated binary outputs (3). The variability in the plantar force patterns between steps is expected in a typical human walk. The corresponding detected gait-phases (2a-e) are graphed in Fig. 9 showing that the algorithm detected the five gait-phases successfully according to the plantar force patterns (Fig. 8). The detected five gait-phases are sequential, and immediately one after another. The relatively repeatable force/time gait cycles and gait-phases show that the normal subject maintains good stability throughout the walking process justifying the choice of a stability function of  $P=1$ .

(3) Table 4 tabulates the average duration and standard deviation (SD) of each phase (normalized to the cycle time of the gait) of the participants on the treadmill at 2km/h. While sharing similar gait patterns, humans walk with their own set of unique gait parameters; thus it is expected that the ground reaction forces would vary from individual to individual.

(4) Table 5 compares the effect of treadmill speeds on the normalized phase-durations. As the treadmill speed has an effect on the walking stability, the subject copes with a higher speed by increasing the relative duration of the MS while shortening the PS in order to maintain the walking stability.

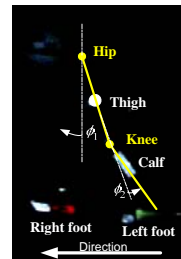
TABLE 4 NORMALIZED PHASE DURATION TO GAIT CYCLE (SPEED = 2 KM/H)

	Phase-duration to gait-cycle ratio (%)				
	$W_{IC}$	$W_{MS}$	$W_{TS}$	$W_{PS}$	$W_{SP}$
Average	7.59	40.82	19.34	4.00	28.25
SD (% of average)	16.4	9.7	25.0	32.5	12.9

TABLE 5 EFFECT OF TREADMILL SPEED ON PHASE DURATION

Subject Weight	Speed (km/h)	Phase-duration to gait-cycle ratio (%)				
		$W_{IC}$	$W_{MS}$	$W_{TS}$	$W_{PS}$	$W_{SP}$
60kg	2.0	6.82	41.17	18.75	3.46	29.8
	2.5	8.27	43.20	13.82	2.89	31.82
	3.0	8.07	44.12	15.35	1.35	30.11

### C. Gait phase and walking kinematics



Normal subject: Male (60kg)  
Treadmill speed =2.5 km/h

Retro-reflective markers  
Hip and knee joints: circular  
Thigh: circular  
Calf and feet: rectangular

Angle measured  
Hip joint angle:  $\phi_1$   
Knee joint angle:  $\phi_2$

Fig. 10 Labeled image showing markers for joint-angle measurements

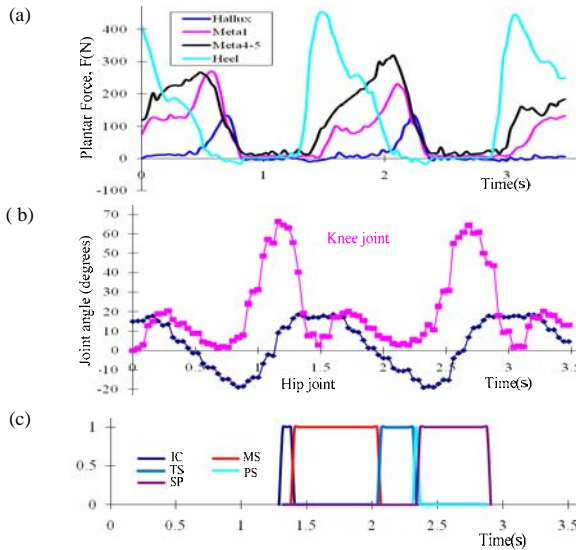


Fig. 11 Relationship among ground reaction forces and joint angles (a) measured plantar forces. (b) Hip and knee joint angles computed from the sequential images (40ms apart). (c) Gait-phases for one walking cycle detected using the threshold algorithm.

To determine the relationship between joint angles during a gait cycle, video images were captured (at 25 frames per second) while the normal subject (Table 5) was walking on the treadmill moving at 2.5km/h. Retro-reflective markers were placed on the hip and knee joints, thigh, calf and feet of the subject (wearing tight-fit pant) as illustrated in Fig. 10.

Figures 11(a) and 11(b) respectively plot the measured plantar forces and the two joint angles computed from the sequential images (40ms apart). For clarity, the detected gait-phases for one gait cycle in Table 5 are also graphed in Fig. 11(c). As shown in Figs. 10(b) and 10(c), the hip angle  $\phi_1$  changes from positive to negative during the mid-stance (MS) phase as the body weight is transferred from the heel to the forefoot. Near the end of the swing phase (SP), the hip angle  $\phi_1$  once again returns to positive to prepare for the next cycle. Because the knee angle  $\phi_2$  is measured from the thigh is fully extended, it is always positive and most active during the swing phase (SP) as expected.

#### IV. CONCLUSION

The feasibility of a walking monitoring shoe (WMS) system for continuous plantar-force measurement and gait-phase detection during walking has been experimentally demonstrated. Results show that the system owns high accuracy and response speed; and video experiment relates gait-phases to the leg kinematics. This simple and affordable method will have potentials for uses by practitioners to assess human gaits and manage patients with foot impairments and foot disorders. It is also potentially a useful tool for scientists to analyze the biomechanics of walking as well as for researchers to

develop human-inspired mechanism for biped robots or exoskeletons.

#### ACKNOWLEDGE

The authors would like to thank Yin Yang for his contribution during the initial period of this project.

#### REFERENCES

- [1] G. P. McComis, D. A. Nawoczinski, and K. E. DeHaven, "Functional bracing for rupture of the Achilles tendon - clinical results and analysis of ground-reaction forces and temporal data," *J. Bone Joint Surg. (Am)*, vol. 79A, no. 12, pp. 1799–1808, Dec. 1997.
- [2] K.-M. Lee and J. Guo, "Kinematic and dynamic analysis of an anatomically-based knee joint," *J. Biomechanics* (in press).
- [3] F. E. Zajac, R. R. Neptune, S. A. Kautzang, "Biomechanics and muscle coordination of human walking. Part I: Introduction to concepts, power transfer, dynamics and simulations," *Gait and Posture* 16, pp. 215–232, 2002.
- [4] Y. Yang, C. J. Yang, K.-M. Lee, and H. Yu, "Model-based Fuzzy Adaptation for Control of a Lower Extremity Rehabilitation Exoskeleton," *IEEE/ASME AIM 2009*, pp. 30–35, Singapore, July 14–17, 2009.
- [5] Q. Huang, K. Yokoi, S. Kajita, K. Kaneko, H. Arai, N. Koyachi, and K. Tanie, "Planning walking patterns for a biped robot," *IEEE Trans Robotics and Automation*, vol. 17, no. 3, pp. 280–289, June 2001.
- [6] M. N. Orlin, and T. G. McPoil, "Plantar pressure assessment," *Phys Therapy*, vol. 80, no. 4, pp. 399–409, 2000.
- [7] A. Faivre, M. Dahan, B. Parratte, and G. Monnier, "Instrumented shoes for pathological gait assessment," *Mechanics Research Communications*, Vol. 31, pp. 627–632, 2004.
- [8] P. H. Veltink, C. Liedtke, E. Droog, and H. Kooij, "Ambulatory measurement of ground reaction forces," *IEEE Trans. Neural Syst. and Rehabil. Eng.*, vol. 13, no. 3, pp. 423–427, Sep. 2005.
- [9] I. P. I Pappas, M. R. Popovic, K. Thierry, V. Dietz, and M. Morari, "A reliable gait phase detection system," *IEEE Trans. Neural Syst. and Rehabil. Eng.*, vol. 9, no. 2, pp. 113–125, 2001.
- [10] M. Chen, B. F. Huang, K. K. Lee, and Y. S. Xu, "An intelligent shoe-integrated system for plantar pressure measurement," *Proc. IEEE Int. Conf. on Robotics and Biomimetics*, pp. 416–421, 2006.
- [11] Y. Okaza, N. Yoshida, and K. Oguchi, "Using sole pressure signals to analyze walking posture," *ICRA2006*, pp. 197–200, 2006.
- [12] C. Lebosse, B. Bayle, M. Mathelin, and P. Renaud, "Nonlinear modeling of low cost force sensors," *ICRA2008*, 3437–3442, 2008.
- [13] G. A. Spolek and F. G. Lippert, "An instrumented shoe-a portable force measuring device," *J. Biomechanics*, 9 (12), 779–783, 1976.
- [14] C. R. Young, "The F-SCAN system of foot pressure analysis," *Clin. Podiatr. Med. Surg.*, vol. 10, no. 3, pp. 455–461, 1993.
- [15] J. Woodburn, and P. S. Helliwell, "Observations on the F-Scan in-shoe pressure measuring system," *Clinical Biomechanics*, vol. 11, no. 5, pp. 301–304, 1996.
- [16] S. Barnett, J. L. Cunningham, and S. West, "A comparison of vertical force and temporal parameters produced by an in-shoe pressure measuring system and a force platform," *Clinical Biomechanics*, vol. 15, no. 4, pp. 781–785, 2000.
- [17] K. Kong and M. Tomizuka, "A gait monitoring system based on air pressure sensors embedded in a shoe," *IEEE/ASME Trans. Mechatronics*, vol. 14, no. 3, pp. 358–370, June 2009.
- [18] F. Vecchi, C. Freschi, S. Micera, A. M. Sabatini, P. Dario and R. Sacchetti, "Experimental evaluation of two commercial force sensors for applications in biomechanics and motor control," *Proc. 5<sup>th</sup> Annual Conf. IFESS 2000*, Jun. 2000.
- [19] G. Yuan, M. X. Zhang, Z. Q. Wang, and J. H. Zhang, "The distribution of foot pressure and its influence factors in Chinese people," *China J. Phys. Med. Rehabil.*, vol. 26, no.3, 156–159, 2004.
- [20] J. Perry, *Gait Analysis: Normal and Pathological Function*, SLACK Inc., 1992.
- [21] Clinical and Research Solutions, Available: <http://www.tekscan.com>